Sb-surfactant-mediated growth of Si and Ge nanostructures

A. Portavoce,[1,2] I. Berbezier,[1,*] and A. Ronda[1]
[1]*CRMC2-CNRS Case 913 Campus de Luminy, 13288 Marseille Cedex 9, France*
[2]*L2MP Faculté des Sciences de St. Jérôme, Case 511, 13397 Marseille, France*
(Received 16 May 2003; revised manuscript received 12 January 2004; published 15 April 2004)

We have used reflection high-energy electron diffraction (RHEED), atomic force microscopy (AFM), and high-resolution electron microscopy (HREM) to investigate Sb surfactant mediated growth (SMG) of Ge on Si. We show that SMG of $Si_{1-x}Ge_x$ promotes the two-dimensional (2D) nucleation regime and increases the critical thickness of the 2D-3D transition at 350 °C. At this temperature, thick defect free flat Ge layers can be epitaxied on 1 ML Sb-Si(001) without formation of Ge islands. At higher temperature (550 °C) Ge islands nucleate after the growth of several 2D monolayers; SMG induces a dramatic reduction of the islands lateral size on both Si(111) and Si(001). We show that the different SMG roles obtained at 350 and 550 °C are explained by the conjunction of thermodynamic and kinetic effects. First we explain the substantial increase of the 2D-3D transition critical thickness by the reduction of Sb induced surface energy. This surface energy reduction has a stabilizing effect of flat $Si_{1-x}Ge_x$ layers (against island growth). Second, we attribute the dramatic reduction of islands size to a lower Ge diffusion length on Sb rich surface. We suggest that this reduced diffusion length is due to the competition between surface diffusion and exchange with subsurface Sb atoms. In addition, Ge:Sb SMG on Si(001) is successfully used for two applications: the growth of flat layers and the self-assembling of ultrasmall, dense and homogeneous Ge dots.

DOI: 10.1103/PhysRevB.69.155416 PACS number(s): 81.16.Dn, 81.07.Ta, 81.10.Aj

I. INTRODUCTION

Several studies report on Sb surfactant mediated growth (SMG) of $Si_{1-x}Ge_x$ on Si. Among the different effects of Sb it was shown that (i) coherent strained flat Ge layers can be grown up to higher critical thickness without relaxation by misfit dislocations,[1–12] (ii) dynamic Ge segregation during growth is reduced[13–14] and Si/Ge intermixing is suppressed,[4,5,10,15–18] (iii) $Si_{1-x}Ge_x$ relaxed buffer layers of better crystalline quality can be obtained (lower density of dislocations and lower surface roughness).[17,19–22] More recently, SMG has also been used for self-organization of Ge islands.[23] In particular, some studies have evidenced a reduction of Ge islands lateral sizes using Sb SMG.[24–26] However, at high temperature, SMG of Ge follows a classical SK regime[2,25] without noticeable influence of Sb.

Although the microscopic mechanism of surfactant effect is still under debate it is generally believed that the main influence of surfactants is to drive the growth in a diffusion-limited regime. In particular, Voigtländer *et al.*[27] have classified surfactant elements in two categories: (i) elements decreasing surface diffusion (As, Sb, Bi, Te) and promoting flat surface and (ii) elements increasing surface diffusion (Sn, Pb, Ga, In) and promoting island formation. Several theoretical[28–30] and experimental[31–32] works have been devoted to the microscopic exchange process of Ge—surfactant rather than to the explanation of the SMG mechanism. Most of them have shown that adatoms/surfactants (As and Sb) use dimmers for the site exchange mechanism. Oh *et al.*,[33] proposed an atomic pushing-out mechanism, which explains the locking of Ge atoms in sub surface sites. This phenomenon is shown to be responsible of the leveling of Ge islands during Sb SMG on Si. Kandel and Kaxiras[34] have shown that surfactants of column V induce a complete passivation of Si. SMG effect is then explained by the different adsorption energies on the terraces and along the step edges.

In addition, it was also suggested that morphological changes induced by SMG could depend on surface reconstruction. For example, Falta *et al.*[35] have shown that while the Ga terminated 6.3×6.3 surface (obtained for Ga coverage $\sim$0.8 ML) promotes 2D layer by layer growth of Ge, the $\sqrt{3}\times\sqrt{3}$-terminated Si(111) surface (obtained for Ga coverage $\sim$1/3 ML) leads to islanding.[36] In the latter case, it is suggested that island nucleation takes place on surface areas locally free of Ga. Recently a work based upon ab initio density functional theory calculations has given thermodynamic evidence of the surfactant aided layer-by-layer growth.[37] The analysis of energetic data of surface free energy as a function of chemical potential was shown to provide a general theoretical signature of the growth mode.

In this study, we compare the morphology of Ge strained layers grown on Si surfaces terminated or not by Sb. We determine the influence of growth temperature (T_G), deposited thickness (h), Sb coverage (θ) and silicon substrate orientation. We find that the driving force of Sb SMG effect comes from the conjunction of thermodynamics and kinetics phenomena. Using basic energetic and kinetic considerations we show a good agreement between the experimental results and the calculated reduction of surface energy and of surface diffusion.

II. EXPERIMENTS

Si and Ge layers were grown on Si(001) and Si(111) substrates in a Riber molecular beam epitaxy (MBE) system, with a base pressure typically $<10^{-11}$ Torr. Si flux was obtained from an electron beam evaporator. Ge and Sb were evaporated from effusion Knudsen cells. Si wafers of nominal orientation (miscut$<0.2°$) were *ex situ* cleaned and protected by an oxide layer as a final step. This oxide layer was

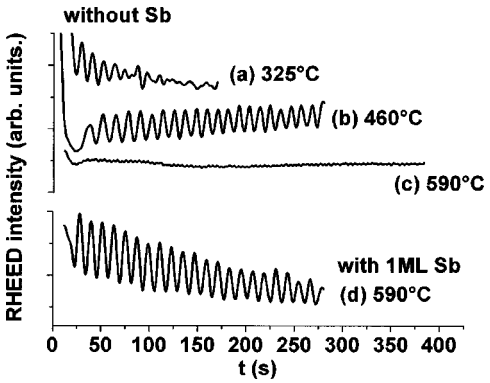

FIG. 1. Variations of the RHEED specular beam intensity during the growth of Si/Si(111) (a)–(c) and Si/1 ML Sb-Si(111) (d).

subsequently removed into the growth chamber by flashing the substrate at 900 °C before performing growth. Reproducible surface is obtained by depositing 50-nm-thick Si buffer layer. Cleanliness of the surface was systematically checked by the observation of reflection high-energy electron diffraction (RHEED) patterns of the 2×1 and 7×7 surface reconstruction [on Si(001) and Si(111), respectively]. Si and Ge were deposited at a rate about 0.3 Å/s and 0.063 Å/s, respectively, directly on the substrate or after the deposition on the surface of a submonolayer coverage of Sb ($0<\theta\leqslant1$). The calibration of the Sb flux was done using the surface reconstruction change from the Si(001)-(2×1) pattern [or Si(111)-(7×7)] to the (1×1) pattern at 1 ML Sb coverage.[38] Calibration using secondary ion mass spectroscopy (SIMS) depth profiles of ~1 ML Sb buried in Si layers was also performed. The morphology of the surface was qualitatively determined during growth by RHEED. Growth regimes were deduced from the RHEED specular beam intensity variations during growth. After growth, atomic force microscopy (AFM) and high-resolution transmission electron microscopy (HRTEM-JEOL 4000 EX) were used for morphological and structural characterization of the deposited layers.

III. RESULTS

A. Si growth

The typical variations of RHEED specular beam intensity as a function of the temperature were recorded during the growth of Si/Si(111) and Si/Sb-Si(111). We find that in the two cases, three main growth regimes can be distinguished: (1) Kinetic roughening at low temperatures. This regime is characterized by an important damping of RHEED oscillations [Fig. 1(a), $T_G=325\,^{\circ}\mathrm{C}$], which is attributed to an increase of surface roughness.[39] The latter is induced by the low surface diffusion of Si adatoms in this growth regime. (2) 2D nucleation (layer-by-layer growth) at intermediate temperatures. This regime is characterized by RHEED oscillations without damping [Fig. 1(b), $T_G=460\,^{\circ}\mathrm{C}$ for Si growth and Fig. 1(d) $T_G=590\,^{\circ}\mathrm{C}$ for SMG]. Growth proceeds by nucleation of 2D islands on the terraces that collapse up to the ML's completion, before the growth of the next ML. (3) Step flow at high temperatures. This regime is evidenced by the total absence of RHEED oscillations [Fig. 1(c), $T_G=590\,^{\circ}\mathrm{C}$]. In this regime, the surface diffusion of Si adatoms is larger than the terrace length and Si adatoms stick to the step edges. Growth proceeds by advancement of the step edges. The temperature of transition between 2D nucleation and step-flow is commonly related to the disappearance of the RHEED oscillations. It corresponds to the temperature at which the diffusion length of adatoms becomes larger than the terraces.

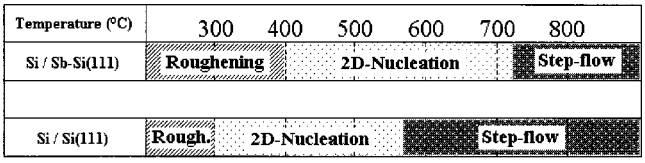

FIG. 2. Schematic evolution of Si/Si(111) and Si/1 ML Sb-Si(111) growth regimes with the temperature.

Figure 2 gives a schematic representation of the three growth regimes evidenced by RHEED during the deposition of Si/Sb-Si(111) and Si/Si(111) as a function of temperature. We first observe a temperature shift towards higher temperatures of the three growth regimes for SMG. This means that the transitions from kinetic roughening to 2D nucleation and from 2D nucleation to step-flow occur at higher temperatures for this system. Since these two transitions are directly related to critical surface diffusion lengths of adatoms, we deduce that Sb induces a decrease of the surface diffusion length. Second, we note that step flow growth regime starts at about 525 °C for normal Si growth while it starts at 725 °C for SMG. Experimental proof of these results is given by the disappearance of RHEED oscillations at temperatures higher than 525 and 725 °C during Si on Si(111) deposition and SMG, respectively. Figures 1(c) and 1(d) show for example the comparison of RHEED oscillations for Si/Si and SMG, respectively, at 590 °C. We must remark that for SMG, the step-flow regime starts at a temperature (725 °C) which corresponds to the peak of thermodesorption of Sb from the Si surface.[40] This means that Si growth proceeds by 2D nucleation on Sb-Si(111) up to almost complete desorption of Sb. We conclude that Sb SMG of Si induces (1) a reduction of the Si adatom diffusion length and (2) the inhibition of step-flow growth. Similar results have been obtained for other SMG systems. For instance, Tromp and Reuter[41] have never observed the step-flow regime during the growth of Ge on the As-terminated Si surface.

B. Ge growth

1. On Si(111) substrate

The variations of the RHEED specular beam intensity have been recorded at two temperatures (350 and 550 °C) during the growth of Ge/Si and Ge/Sb-Si. All the experiments have been stopped after the growth of ~7 ML (~2.2 nm) in order to analyze the RHEED patterns and the morphology of the as grown surfaces.

At 350 °C during the growth of Ge/Si, three oscillations can be observed [Fig. 3(a)]. They are attributed to the layer-by-layer growth of Ge during 3 ML's (~1 nm) followed by

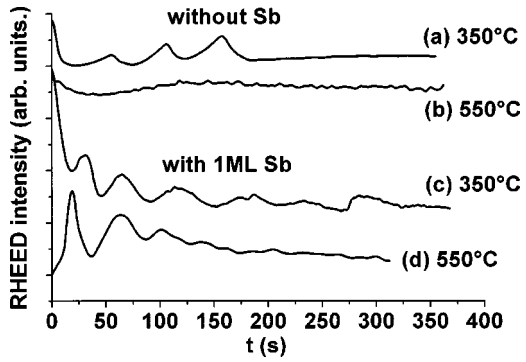

FIG. 3. Variations of the RHEED intensity during the growth of Ge/Si(111) (a), (b) and Ge/1 ML Sb-Si(111) (c), (d).

3D growth of islands. This growth process of Ge/Si is already well known. Moreover, formation of islands is confirmed by the transformation from streaks to spots observed on the RHEED pattern at the end of the growth experiment [Fig. 4(a)]. At 550 °C, we can note the total absence of RHEED oscillations [Fig. 3(b)]. This is consistent with the step flow growth regime expected at this temperature. After the growth, the RHEED pattern presents the typical 5×5 reconstruction of Ge deposits on Si(111) (Ref. 25) [Fig. 4(b)]. The RHEED pattern evidences a flat surface, although we will see in the next section that it consists of very large flat islands. This discrepancy is due to the low coherence length of RHEED which prevents to distinguish islands when they are large and flat and a totally flat surface.

During Sb SMG of Ge: at 350 °C, six RHEED oscillations are now observed [Fig. 3(c)]. They are attributed to the layer-by-layer growth of 6 ML's Ge (~1.9 nm): two times larger than without Sb. The 2D growth is confirmed by the presence of streaks on the RHEED pattern at the end of the growth [Fig. 4(c)]. At 550 °C three oscillations are observed [Fig. 3(d)]. This suggests the growth of 3 ML's by 2D nucleation followed by the growth of 3D islands. Formation of islands is confirmed by the presence of spots on the RHEED pattern at the end of the growth [Fig. 4(d)]. At this growth temperature, in the case of Ge deposition without Sb, we did not observed 2D nucleation. We then deduce that this growth regime results from SMG on the Sb-terminated surface. It is attributed to a reduced surface diffusion length of Ge adatoms. Consequently, from this set of experiments we find that Sb SMG of Ge induces (1) a decrease of Ge adatom diffusion length and (2) an increase of the critical thickness (h_{cr}) of the 2D-3D transition; at 350 °C, $h_{cr}\sim6$ ML's for Ge/Sb-Si instead of $h_{cr}\sim3$ ML's for Ge/Si.

Regarding now the morphology of the as-grown surfaces, they are strongly different when Ge is deposited on Si(111) and when it is deposited on Sb-Si(111) as can be seen on the

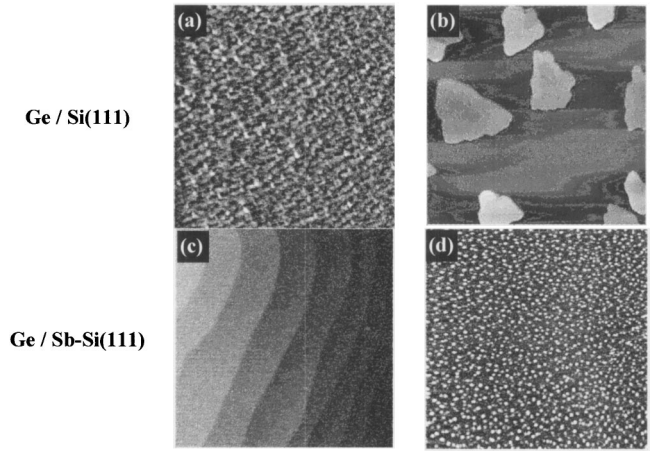

FIG. 5. AFM images of the surface after deposition of Ge/Si(111) at $T_G=350$ °C (a) and $T_G=550$ °C (b) and Ge/1 ML Sb-Si(111) at $T_G=350$ °C (c) and $T_G=550$ °C (d). At 350 °C 2D layers are obtained (scan of the image is 2×2 μm^2) while at 550 °C islands have formed (scan size of the images is 4×4 μm^2).

AFM images presented in Fig. 5. Table I summarizes the typical features of the different morphologies deduced from AFM observations. After the growth of ~7 ML's of Ge, we observe at 350 °C small Ge islands on Si [Fig. 5(a)] and an atomically flat surface on Sb-Si [Fig. 5(c)]; the regular train of biatomic steps resulting from the small miscut (~0.1°) of the initial surface is in particular still visible. At higher temperature (550 °C), we observe very large flat Ge islands on Si [Fig. 5(b)] and much smaller islands (size ~20 times smaller and density ~500 times larger) on Sb-Si [Fig. 5(d)]. RHEED oscillations (not shown here) confirm the AFM results. It is deduced that Sb SMG of Ge induces an increase of h_{cr} 2D-3D transition and a decrease of the adatoms surface diffusion length.

2. On Si(001) substrate

In this part we focus on the morphological evolution of Ge layers with growth temperature (T_G), deposited thickness (h), and Sb coverage (θ).

Evolution with T_G. Figure 6 shows the morphology of Ge layers obtained at three growth temperatures $T_G=350$, 550, and 750 °C, for $\theta=1$ and $h\sim13$ ML (~1.8 nm). At 350 °C [Fig. 6(a)], the surface is flat with a root mean square roughness r.m.s.~0.5 nm. HRTEM observations [Fig. 6(d)] evidence an atomically flat film, free of dislocations and fully strained to the Si substrate. At 550 °C [Fig. 6(b)], the layer consists of ultrasmall islands ($\varnothing\sim30$ nm, $h\sim1$ nm, $d\sim1.5\times10^{11}/cm^2$) free of dislocations. They are closely packed but not in contact with each other (mean distance between

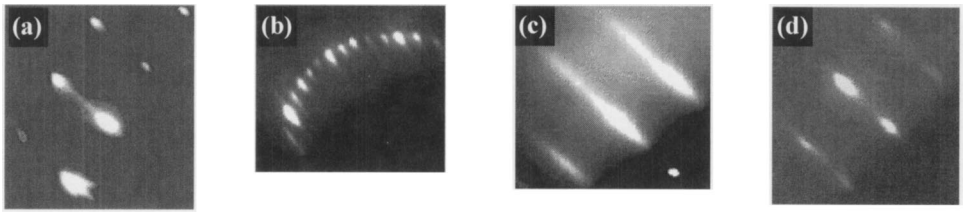

FIG. 4. RHEED patterns after deposition of Ge/Si(111) at $T_G=350$ °C (a) and $T_G=550$ °C (b) and Ge/1 ML Sb-Si(111) at $T_G=350$ °C (c) and $T_G=550$ °C (d). In all cases deposited thickness of Ge is ~7.5 ML.

TABLE I. Typical features of Ge surface morphologies obtained at 350 and 500 °C on Si and Sb-Si surfaces. r.m.s. represents the root mean square roughness of the 2D layers. h, $\varnothing$, and d represent the height, diameter, and density of the 3D islands.

	350 °C	550 °C
Ge/Si	2D rough layer r.m.s.~1 nm	3D islands $h=10$ nm, $\varnothing=1500$ nm, $d\sim 2.10^7/\text{cm}^2$
Ge/Sb-Si	2D layer r.m.s.~0.2 nm	3D islands $h=5$ nm, $\varnothing=80$ nm, $d\sim 9.10^9/\text{cm}^2$

island edges ~5 nm) as can be seen on the TEM cross-section image [Fig. 6(e)]. At 750 °C [Fig. 6(c)] low density of large dislocated Ge islands with rounded shape is observed ($\varnothing\sim 230$ nm, $h\sim 60$ nm, and $d\sim 3\times 10^8/\text{cm}^2$). These islands are usually called ''domes'' and are frequently observed during the growth of Ge on Si (without Sb coverage).[42,43] A typical TEM cross-section image of such an island is presented in Fig. 6(f). The similarity of Ge island morphology when Ge is deposited on Sb-Si and on Si substrates at this growth temperature is explained by the absence of Sb on the surface due to the desorption of Sb at ~700 °C (Ref. 40) from Ge(001).

Evolution with h. We have then investigated the morphological evolution of Ge layers with the deposited thickness at 550 °C for $\theta=1$. AFM images of Ge layers with thicknesses of (a) 0.9 nm, (b) 1.2 nm, (c) 1.8 nm, and (d) 2.7 nm are presented in Fig. 7. The growth processes can be divided in three steps: (1) layer-by-layer growth up to $h\sim 0.9$ nm, (2) nucleation of 3D islands (and increase of island density) up to $h\sim 1.8$ nm, and (3) coalescence of islands. The maximum of islands density is obtained at $h\sim 1.8$ nm (Fig. 8). One can also note the almost constant size of islands up to the merging step ($25\text{ nm}\leqslant\varnothing\leqslant 30$ nm).

Evolution with θ. We have compared the morphology of Ge layers 13-ML thick obtained at 550 °C for $\theta=0$, 0.5, and 1. We observe a strong reduction of island size (accompanied by a higher density of islands) when increasing θ (Fig. 9); this is clearly visible on the AFM images [Figs. 10(a), 10(b), and 7(c) for $\theta=0$, 0.5, and 1, respectively]. One can also notice the effect of Sb predeposition on Ge island shape. Regarding first Ge/Si growth, as already described in several papers,[44–47] a bimodal size distribution of islands is obtained [Fig. 10(a)]. The islands consist of ''huts'' with {105} facets and ''domes'' with mainly {111} and {113} facets. The {105} facets are clearly identified by TEM cross-section observations [Fig. 10(c)]. While huts are strained (no dislocation), most of the domes are relaxed. When Ge is deposited on Sb-Si, a dramatic change of island shape is observed [Fig. 10(b)]. First, only one type of island free of dislocations with a rounded shape is now observed. Second, the islands no longer present a visible facet on their top or their sides [Fig. 10(d)]. This suggests that surface energy anisotropy of Ge is also modified by Sb adsorption.

In summary, we have shown in this part that Sb SMG of Ge induces a change of island shape (with in particular the disappearance of facets) and a dramatic reduction of their lateral size accompanied by the increase of their density. At high temperature, there is no surfactant effect because of Sb desorption.

IV. DISCUSSION

In this study we have performed growth experiments on both Si(111) and Si(100) in order to determine the role of surface reconstruction on Sb SMG. Indeed, it is known[2,48] that the reconstructions stabilized at the Sb-Si(001) and Sb-Si(111) surfaces are different despite the 1×1 RHEED pattern observed after 1 ML Sb deposition in the two cases.

We have found similar effects of submonolayer coverages of Sb on the growth of Si and of Ge. These effects have been evidenced for two different surface reconstructions [on (111) and on (001)] and in two different growth regimes (2D nucleation and step flow).

All the Ge layers investigated on Si(001) were free of dislocations (in the limit of sensitivity of TEM measurements) and were consequently completely strained up to a thickness of 1.8 nm (13 ML). We then can conclude that the critical thickness (h_c) is higher than 13 ML for Sb SMG on Si(001).

We have evidenced different effects of Sb SMG depending on the temperature: at low temperature, delay of the 2D-3D growth transition and inhibition of the step-flow growth regime; at high temperature, a dramatic reduction of Ge island size accompanied by an increase of their density

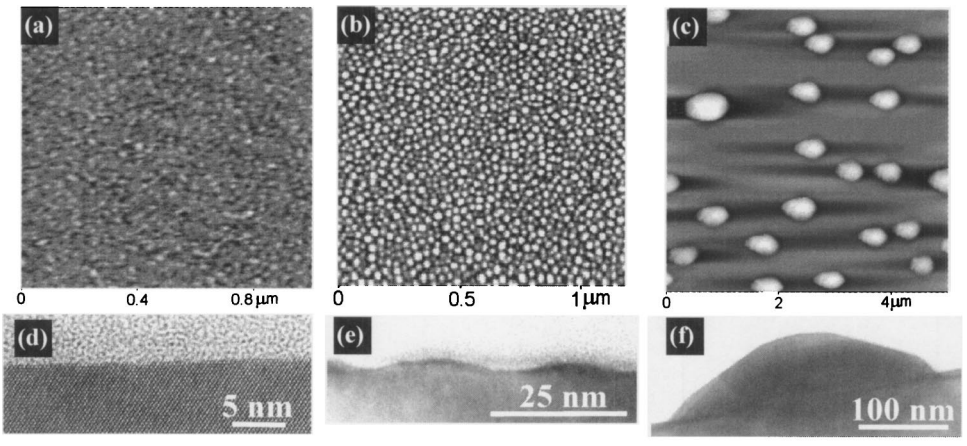

FIG. 6. Images of the surface after the growth of 13 ML Ge/1 ML Sb-Si(001) at 350 °C (a) and (d), 550 °C (b) and (e), and 750 °C (c) and (f). (a)–(c) images are AFM images and (d)–(f) are TEM cross-section images. In (a), (b) the scan of the images is $1\times 1\ \mu\text{m}^2$, in (c) scan size is $5\times 5\ \mu\text{m}^2$.

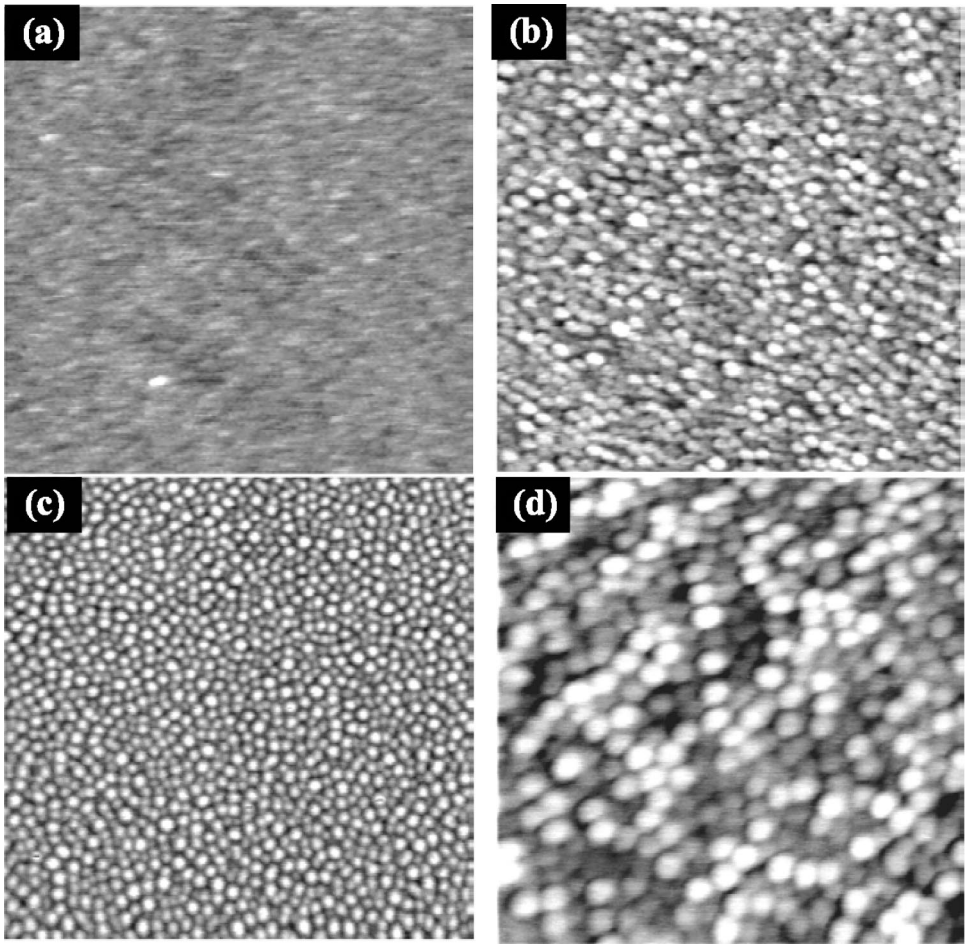

FIG. 7. AFM images of Ge/1 ML Sb-Si(001) obtained at 550 °C for deposited thicknesses of (a) 9 Å, (b) 12 Å, (c) 18 Å, and (d) 27 Å [scan size of the images is $1\times1\ \mu m^2$].

and by a modification of island shape (with in particular the absence of visible facets). We suggest that these effects can be interpreted as the combination of two driving forces: (i) thermodynamic,[2,24,37] the decrease of surface energy induced by Sb submonolayer coverages which promotes 2D growth and (ii) kinetic, the decreases of adatoms diffusion length due to the competition between surface diffusion and exchange with Sb atoms of the subsurface which reduces the island size.

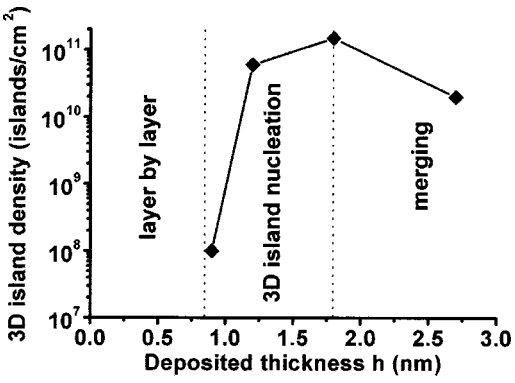

FIG. 8. Evolution of the 3D islands density with the Ge deposited thickness for growth at 550 °C on 1 ML Sb-Si(001).

A. Thermodynamic driving force

The critical thickness of 2D-3D transition (h_c) corresponds to the minimisation of the total free energy of the system (E). By approximation, if E only consists of two terms, surface energy (γ) and elastic energy (E_{el}), then h_c corresponds to the thickness at which the reduction of elastic energy induced by relaxation at step edges in the islands becomes larger than the excess of surface energy induced by the larger surface developed by the islands. Now if we compare the cases of a Ge layer in epitaxy on a Si substrate

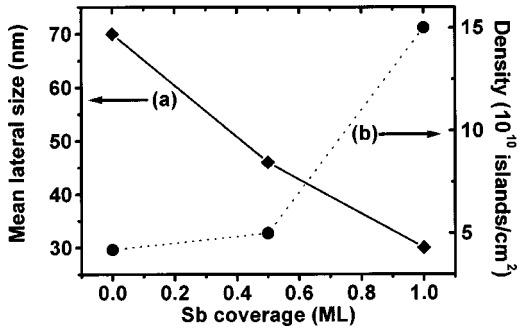

FIG. 9. Evolution of the mean lateral size of islands (a) and of their surface density (b) with Sb coverage.

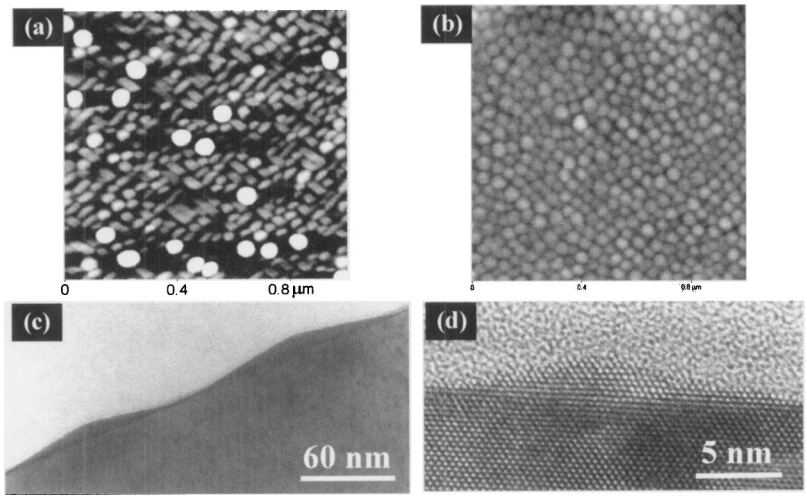

FIG. 10. AFM (a), (b) and TEM (c), (d) images of 13 ML Ge/θ ML Sb-Si(001) obtained at 550 °C with $\theta=0$ (a) and (c), $\theta=1/2$ (b), and $\theta=1$ (d).

(Ge/Si) and of a Ge layer covered with a submonolayer of Sb (Sb:Ge/Si), at the 2D-3D transition the total critical free energy (E_c) is the same in the two cases [$\Delta E_c(h_c)=0$]. We can write at constant temperature

$$\Delta\gamma(\theta)+\Delta E_{\mathrm{el}}(h_c)=0, \tag{1}$$

where $\Delta\gamma(\theta)$ and $\Delta E_{\mathrm{el}}(h_c)$ are the surface energy and elastic energy differences between Ge/Si and Sb:Ge/Si structures. The variations of the volume and of the chemical potential of the crystal are neglected in Eq. (1) as the silicon substrate can be considerate as semi-infinite. Neglecting the possible changes of the microscopic surface state (surface reconstruction, roughness, etc.), it is reasonable to assume that the surface energy follows a Vegard's law with Sb coverage (θ):

$$\gamma(\theta)=\theta\gamma^{\mathrm{Sb}}+(1-\theta)\gamma^{\mathrm{Ge}} \tag{2}$$

with γ^{Sb} and γ^{Ge} the surface energy of Sb and Ge.

The elastic energy (E_{el}) stored in the flat Ge layer epitaxied on the Si substrate is calculated using the classical equation

$$E_{\mathrm{el}}(h)=2\mu\frac{1+\nu}{1-\nu}\varepsilon^2 V \quad \text{with} \quad V=Sh, \tag{3}$$

where μ and ν are the shear modulus and the Poisson's ratio of Ge; ε is the lattice misfit between Ge and Si; V is the volume of the Ge layer and S the surface area of the crystal. Again the influence of the microscopic surface state is neglected in E_{el}.

We experimentally measured $h_c=3$ ML for $\theta=0$ on Si(111) at 350 °C. From Eqs. (2) and (3) (and considering $\gamma^{\mathrm{Si(001)}}/\gamma^{\mathrm{Si(111)}}\sim 1.1$ as found experimentally) we deduced $h_c=4$ ML for $\theta=0$ on Si(001). Using these values we have calculated h_c versus θ. The results are presented on Fig. 11. We can see a good agreement between the calculations and the experimental results of Katayama *et al.*[4] on Si(001) and our experimental results on (111) at low temperature. This description explains the increase of the critical thickness for the 2D-3D transition observed experimentally at low temperature during Sb SMG.

However, at higher temperature (550 °C), some discrepancies exist at $\theta\sim 1$, between the estimation of $h_c\sim 17$ ML (on 001) and the experimental value that we have found ($h_c\sim 7$ ML). Also, Horn-von Hoegen *et al.*[24] ($T_G=700$ °C), Voigtländer and Zinner[2,25] ($T_G>600$ °C) and Peng *et al.*[26] ($T_G=550$ °C) have evidenced the formation of islands at much lower h_c. We suggest that Sb partial desorption during growth of Ge is responsible of this effect. Indeed, it has been shown that Sb desorption during growth of $Si_{0.8}Ge_{0.2}$ at 550 °C is much larger than those predicted by the thermodynamic data.[40,49] In Ref. 49 we measured a desorption rate $K_d\sim 6.3\times 10^{-3}$ s^{-1} during the growth of $Si_{0.8}Ge_{0.2}$ at 550 °C. If we assume that Sb desorption from SiGe and Ge is of the same order (as shown in Ref. 40), we deduce that $\theta\sim 1/3$ (instead of 1) at the end of the Sb SMG of Ge at 550 °C. Taking into account this desorption, we now find a good agreement between $h_{\mathrm{cr}}\sim 8$ ML (estimated at $\theta\sim 1/3$) and the experiments ($h_c\sim 7$ ML). In consequence, we explain the formation of islands at $T_G\geqslant 550$ °C on Sb:Si(001) and Sb:Si(111) by the partial desorption of Sb.

In summary, at low temperature, when there is no Sb desorption the experimental h_c is in good agreement with the calculated values. At higher temperature, the smaller h_c measured experimentally is explained by Sb partial desorption.

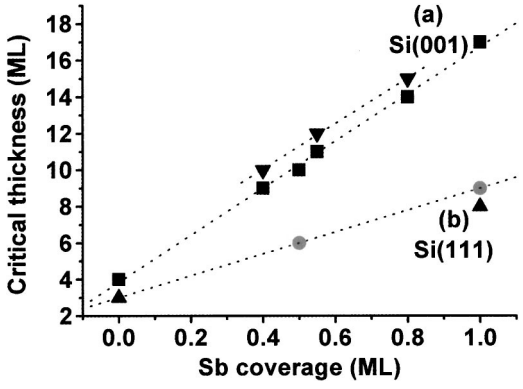

FIG. 11. Evolution of the critical thickness of the 2D-3D growth transition with Sb coverage on Si(001) (a) and on Si(111) (b). Up and down triangles represent experimental values.

Indeed, the linear increase of surface energy with Sb desorption [as described in Eq. (2)] promotes island formation. We then conclude that above a critical Sb coverage, the Ge layer relaxes strain directly by nucleating dislocations without formation of 3D islands. This is what we observe at low temperature. This interpretation is based on purely macroscopic thermodynamic arguments. It permits us to explain the morphology evolution of Ge layers versus growth temperature, as well as the decrease of the wetting layer thickness when the temperature increases.

B. Kinetic driving force

The coefficient of diffusion (D) for a cubic lattice can be written

$$D \approx a^2 Z \nu \exp\left(\frac{-E}{kT}\right). \tag{4}$$

Z, a, ν, E, k, and T are the number of neighbor sites, the distance between neighbor sites, the Debye frequency, the activation energy, the Boltzmann constant, and the temperature, respectively. We express the mean surface diffusion coefficient (D_{SD}) of Ge adatoms as

$$D_{SD} = a^2 Z_s \nu_s \left\{ \theta \exp\left(\frac{-E_{SD}^{\mathrm{Sb}}}{kT}\right) + (1-\theta)\exp\left(\frac{-E_{SD}^{\mathrm{Ge}}}{kT}\right)\right\}, \tag{5}$$

where E_{SD}^{Sb} and E_{SD}^{Ge} are the activation energies of the Ge adatom diffusion on a Sb and a Ge surface, respectively.

Because of the dynamic segregation of Sb during growth, another mechanism has to be considered: the two sites exchange between adatoms and Sb atoms located in the subsurface layer. As a consequence, when an atom is deposited on the surface, it can either diffuse, or exchange with Sb subsurface atoms. The exchange rate (Γ_{ex}) can be defined as

$$\Gamma_{\mathrm{ex}} = \theta \nu_\nu \exp\left(-\frac{E_{\mathrm{ex}}}{kT}\right). \tag{6}$$

Considering that the phonon vibrations at the surface are generally twice as important as the bulk ones ($\nu_s = 2\nu_\nu$), the diffusion time (τ) of Ge adatoms before to exchange with Sb subsurface atoms is then

$$\tau = \frac{1}{\Gamma_{\mathrm{ex}}} = \frac{2}{\theta \nu_s} \exp\left(\frac{E_{\mathrm{ex}}}{kT}\right). \tag{7}$$

The Ge adatom diffusion length on the surface ($\lambda = \sqrt{D_{SD}\tau}$) can be expressed as

$$\lambda = a\sqrt{2Z_s}\left[\exp\left(\frac{E_{\mathrm{ex}} - E_{SD}^{\mathrm{Sb}}}{kT}\right) + \frac{(1-\theta)}{\theta}\exp\left(\frac{E_{\mathrm{ex}} - E_{SD}^{\mathrm{Ge}}}{kT}\right)\right]^{1/2}. \tag{8}$$

In the case of $\theta = 1$, Eq. (8) gives

$$\lambda = a\sqrt{2Z_s}\left[\exp\left(\frac{E_{\mathrm{ex}} - E_{SD}^{\mathrm{Sb}}}{kT}\right)\right]^{1/2}. \tag{9}$$

We can reasonably assume that the energetic barriers of the Ge surface diffusion and of the Sb surface segregation are in the same range with $E_{\mathrm{ex}} \geqslant E_{SD}^{\mathrm{Sb}}$ (the barrier of interplan atomic exchanges is expected to be larger than the barrier of atomic jump on the surface). In the limit case of $E_{\mathrm{ex}} = E_{SD}^{\mathrm{Sb}}$ (at $\theta = 1$) we obtain the minimal value of $\lambda = a\sqrt{2Z_s}$ from Eq. (9).

The evolution of λ in Eq. (8) explains the reduction of Ge island size when Sb coverage increases: when θ decreases the diffusion length increases (the second term of λ increases). At $\theta = 1$, the diffusion length is directly related to $E_{\mathrm{ex}} - E_{SD}^{\mathrm{Sb}}$ [see Eq. (9)]: lower is the activation energy of exchange, lower is λ and consequently lower is the island size. In conclusion, considering equilibrium thermodynamics or kinetics, the island formation at 550 °C is explained by the partial desorption of Sb during growth.

V. CONCLUSION

We have shown that the predeposition of a submonolayer of Sb before Ge MBE growth permits us to (i) at low temperature (350 °C), increase the critical thickness of the 2D-3D growth transition and (ii) at higher temperature (550 °C), to control Ge island size, shape and density (reduction of islands size, increase of surface density and modification of shape). We explain these two effects by the decrease of both the surface energy and the surface diffusion length during Sb SMG of Ge. We have shown that both equilibrium (surface energy/elastic energy) and kinetics (surface diffusion/surface segregation) considerations explain the island formation at 550 °C by the partial desorption of Sb. The Sb:Ge SMG process developed in this study can be used for two applications: the growth of highly concentrated $Si_{1-x}Ge_x$ flat layers in epitaxy on Si, or the self-assembling of very small Ge dots with a high surface density.

ACKNOWLEDGMENT

The EC project FORUM FIB (Grant No. IST-2000-29574) is acknowledged for financial support.

*Email address: berbezier@crmc2.univ-mrs.fr

[1] K. Sakamoto, K. Miki, T. Sakamoto, H. Matsuhata, and K. Kyoya, J. Cryst. Growth **127**, 392 (1993).

[2] B. Voigtländer and A. Zinner, J. Vac. Sci. Technol. A **12**, 1932 (1993).

[3] M. Horn-von Hoegen, B. H. Müller, and A. Al-Falou, Phys. Rev. B **50**, 11 640 (1994).

[4] M. Katayama, T. Nakayama, M. Aono, and C. F. McConville, Phys. Rev. B **54**, 8600 (1996).

[5] S. Nilsson, H. P. Zeindl, D. Krüger, J. Klatt, and R. Kurps, in *Evolution of Epitaxial Structure and Morphology*, edited by A. Zangwill *et al.*, Mater. Res. Soc. Symp. Proc. No. 399 (Materials Research Society, Warrendale, 1996), p. 197.

[6] I. Davoli, R. Gunnella, R. Bernardini, and M. De Crescenzi, J. Electron Spectrosc. Relat. Phenom. **83**, 137 (1997).

[7] S. Dreiner, C. Westphal, F. Sökeland, and H. Zacharias, Appl.

Surf. Sci. **123/124**, 610 (1998).
[8] P. Zahl, P. Kury, and M. Horn von Hoegen, Appl. Phys. A: Mater. Sci. Process. **69**, 481 (1999).
[9] P. Castrucci, R. Gunnella, N. Pinto, R. Bernardini, M. De Crescenzi, and M. Sacchi, Surf. Rev. Lett. **7**, 307 (2000).
[10] R. Gunnella, P. Castrucci, N. Pinto, I. Davoli, D. Sébilleau, and M. De Crescenzi, Phys. Rev. B **54**, 8882 (1996).
[11] H. Zhu, Z. Jiang, A. Xu, M. Mao, D. Hu, X. Zhang, X. Liu, D. Huang, X. Wang, J. Sun, M. Li, and X. Jiang, J. Cryst. Growth **179**, 115 (1997).
[12] J. R. Power, K. Hinrichs, S. Peters, K. Haberland, N. Esser, and W. Richter, Phys. Rev. B **62**, 7378 (2000).
[13] H. P. Zeindl, S. Nilsson, J. Klatt, D. Krüger, and R. Kurps, J. Cryst. Growth **157**, 31 (1995).
[14] G. G. Jernigan, C. L. Silvestre, M. Fatemi, M. E. Twigg, and P. E. Thompson, J. Cryst. Growth **213**, 299 (2000).
[15] Z. Jiang, A. Xu, D. Hu, H. Zhu, X. Liu, X. Wang, M. Mao, X. Zhang, J. Hu, D. Huang, and X. Wang, Thin Solid Films **321**, 116 (1998).
[16] M. E. Gonzàlez-Méndez and N. Takeuchi, Surf. Sci. **441**, L897 (1999).
[17] S. Kanakaraju, A. K. Sood, and S. Mohan, Phys. Rev. B **61**, 8334 (2000).
[18] P. Castrucci, R. Gunnella, N. Pinto, R. Bernardini, M. De Crescenzi, and M. Sacchi, Surf. Rev. Lett. **7**, 307 (2000).
[19] D. Reinking, M. Kammler, M. Horn-von Hoegen, and K. R. Hofmann, Appl. Phys. Lett. **71**, 924 (1997).
[20] M. Kammler, D. Reinking, K. R. Hofmann, and M. Horn-von Hoegen, Thin Solid Films **336**, 29 (1998).
[21] J. L. Liu, C. D. Moore, G. D. U'Ren, Y. H. Luo, Y. Lu, G. Jin, S. G. Thomas, M. S. Goorsky, and K. L. Wang, Appl. Phys. Lett. **75**, 1586 (1999).
[22] J. L. Liu, S. Tong, Y. H. Luo, J. Wan, and K. L. Wang, Appl. Phys. Lett. **79**, 3431 (2001).
[23] B. Voigtländer and N. Theuerkauf, Surf. Sci. **461**, L575 (2000).
[24] M. Horn-von Hoegen, B. H. Müller, A. Al-Falou, and M. Henzler, Phys. Rev. Lett. **71**, 3170 (1993).
[25] B. Voigtländer and A. Zinner, Surf. Sci. **351**, L233 (1996).
[26] C. S. Peng, Q. Huang, W. Q. Cheng, J. M. Zhou, Y. H. Zhang, T. T. Sheng, and C. H. Tung, Appl. Phys. Lett. **72**, 2541 (1998).
[27] B. Voigtländer, A. Zinner, T. Weber, and H. P. Bonzel, Phys. Rev. B **51**, 7583 (1995).
[28] B. D. Yu and A. Oshiyama, Phys. Rev. Lett. **72**, 3190 (1994).
[29] T. Ohno, Phys. Rev. Lett. **73**, 460 (1994).
[30] M. A. Boshart, A. A. Bailes III, and L. E. Seiberling, Phys. Rev. Lett. **77**, 1087 (1996).
[31] B. D. Yu, T. Ide, and A. Oshiyama, Phys. Rev. B **50**, 14 631 (1994).
[32] A. A. Bailes III, M. A. Boshart, and L. E. Seiberling, Nucl. Instrum. Methods Phys. Res. B **136-138**, 804 (1998).
[33] C. W. Oh, E. Kim, and Y. H. Lee, Phys. Rev. Lett. **76**, 776 (1996).
[34] D. Kandel and E. Kaxiras, Phys. Rev. Lett. **75**, 2742 (1995).
[35] J. Falta, M. Copel, F. K. LeGoues, and R. M. Tromp, Appl. Phys. Lett. **62**, 2962 (1993).
[36] J. Falta, T. Schmidt, A. Hille, and G. Materlik, Phys. Rev. B **54**, R17 288 (1996).
[37] S. J. Jenkins and G. P. Srivastava, Surf. Sci. **398**, L308 (1998).
[38] D. A. Grützmacher, K. Eberl, A. R. Powell, B. A. Ek, T. O. Sedgwick, and S. S. Iyer, Thin Solid Films **225**, 163 (1993).
[39] B. Gallas, I. Berbezier, and J. Derrien, Thin Solid Films **294**, 69 (1997).
[40] A. Portavoce, F. Bassani, A. Ronda, and I. Berbezier, Surf. Sci. **519**, 185 (2002).
[41] R. M. Tromp and M. C. Reuter, Phys. Rev. Lett. **68**, 954 (1992).
[42] I. Berbezier, A. Ronda, and A. Portavoce, J. Phys.: Condens. Matter **14**, 8283 (2002).
[43] I. Berbezier, A. Ronda, F. Volpi, and A. Portavoce, Surf. Sci. **531**, 231 (2003).
[44] A. Ronda, I. Berbezier, A. Pascale, A. Portavoce, and F. Volpi, Mater. Sci. Eng., B **101**, 95 (2003).
[45] F. Volpi, A. Portavoce, A. Ronda, Y. Shi, J. M. Gay, and I. Berbezier, Thin Solid Films **380**, 46 (2000).
[46] M. Goryll, L. Vescan, K. Schmidt, S. Mesters, H. Lüth, and K. Szot, Appl. Phys. Lett. **71**, 410 (1997).
[47] G. Medeiros-Ribeiro, A. M. Bratkovski, T. I. Kamins, D. A. Ohlberg, and R. S. Williams, Science **279**, 353 (1998).
[48] M. Richter, J. C. Woicik, J. Nogami, P. Pianetta, K. E. Miyano, A. A. Baski, T. Kendelewicz, C. E. Bouldin, W. E. Spicer, C. F. Quate, and I. Lindau, Phys. Rev. Lett. **65**, 3417 (1990).
[49] A. Portavoce, F. Volpi, A. Ronda, P. Gas, and I. Berbezier, Thin Solid Films **380**, 164 (2000).